Atomic structure and chemical composition analysis of the (100) surface of the In_3Ni_2 intermetallic catalyst

Tom Bonnar
201542172

A thesis submitted in partial fulfilment of the requirements for the degree of
Bachelor of Science

Under the supervision of Dr. Hem Raj Sharma
at the
Department of Physics

May 6, 2025

Contents

DECLARATION

I declare that the work in this dissertation is my own, and has not been submitted anywhere for any award. Where sources of information have been used, they have been acknowledged.

6/5/2024

ACKNOWLEDGMENTS

I would like to thank my project supervisor, Dr. Hem Raj Sharma, who has been an invaluable help over the course of this project. I would also like to thank Ahowd Youssef Alfahad, who provided me with the data to analyse, as well as provided a great amount of advice which aided my project. Finally, I would like to thank Dr. Sam Coates, Prof. Rowan McGrath, Ellie Weightman and Liam Chandler, who have all been incredibly kind and hospitable during my short time at the SSRC.

Abstract

Intermetallic compounds have shown better selectivity and thermal stability during catalysis when compared to metallic catalysts in the same reactions. These properties suggest they are promising replacements for the expensive and environmentally unfriendly metallic catalysts currently in use. Understanding the atomic structure and chemical composition of the catalytic surface of intermetallic catalysts is therefore vital for further optimising their performance. In this dissertation I have investigated the intermetallic compound In_3Ni_2 using scanning tunneling microscopy (STM), low-energy electron diffraction (LEED) and x-ray photoelectron spectroscopy, which all provide results that can be analysed to understand the characteristics of the (100) surface layer. The In_3Ni_2(100) atomic surface was cleaned with repeated cycles of sputtering and annealing within ultra-high vacuum conditions, and displayed a (1 x 1) LEED pattern afterwards. The step heights observed by STM are consistent with the lattice constant. STM atomic resolution analysis produced lattice parameters of 4.40 $\pm$ 0.1 Å and 5.29 $\pm$ 0.1 Å, which are also consistent with known values for atomic spacing between In atoms. Both step heights and high resolution images indicate the surface termination at the pure In plane, where In atoms are bonded with Ni on the layer below. Based on the STM results and known surface energies it was found that the surface In atoms are likely to have intermetallic bonds with Ni, stabilising the atomic surface. XPS chemical composition analysis indicated a higher proportion of Ni at the surface compared to the bulk composition, indicating promising catalytic potential.

1 Introduction

Intermetallic compounds (IMCs) are compounds with two or more constituent elements occupying specific sites within their crystal structure. Unlike other compounds with multiple constituent elements such as alloys, IMCs have specific stoichiometry, which suggest they are promising candidates to replace metal catalysts in heterogeneous catalysis. In addition, their constituent elements are lower cost and more environmentally friendly to produce than their metal catalyst counterparts [1,2].

IMCs form crystals which are fully or partially ordered and have atomic structures distinct from their constituent elements. Both ionic and covalent bonds are present within their structure, and the free electrons within the compound result in unique electronic and crystal structures. By altering the chemical composition of IMCs, the compound's electronic properties can be adjusted for specific needs as a catalyst. Furthermore, the spatial separation between active sites within IMCs results in better thermal stability and selectivity than metallic catalysts, as observed in Pd-Ga IMCs in hydrogenation reactions[3-5].

The motivation behind this project was to determine the chemical composition and atomic structure of In_3Ni_2 to understand how to optimise it for catalysis. In-Ni IMCs have already been found to be more environmentally friendly and effective in the dry reforming of methane, which converts two major greenhouse gases into hydrogen and syngas, than the previously used nickel-based catalysts. Catalytic activity and selectivity are dependent on the chemical composition of the compound and particle size, with In_3Ni_2 being found to be a particularly high performing catalyst as a result of the electron transfer and active-site isolation present within the compound [5,6].

1.1 Objectives

Over the course of this project, I aimed to study the (100) surface of the In_3Ni_2 intermetallic catalyst to determine the atomic structure and the chemical composition of the compound. To achieve this, a number of processes were employed, including scanning tunneling microscopy and low-energy electron diffraction to characterise surface atomic structure, and x-ray photoelectron spectroscopy to characterise surface chemical composition.

2 Methods

2.1 Apparatus and Sample Details

2.1.1 UHV

Ultrahigh vacuum conditions are enclosures designed to produce a pressure range of below 10^{-9} Torr [7]. The use of UHV conditions are vital in surface science experimentation to avoid contamination of the surface from otherwise ambient gases, prompting uncontrolled reactions such as oxidation to occur within the chamber. Furthermore, it is necessary to avoid ambient gas molecules in the chamber from interfering with the probe and detected surface particles, affecting the collected data.

An example of a UHV chamber is displayed in Figure 1. The chambers are built of stainless steel, and consist of a roughing pump to lower the pressure to ranges of around $10^{-}3$ Torr, and a high vacuum pump (such as an ion or cryogenic pump) to reach UHV levels. UHV systems are baked out to prevent outgassing, where they are heated to between 150-250°C for several hours, which accelerations desorption of gases from the chamber walls [8].

2.1.2 Sample Preparation and Measurements

The compound used for this study was a single crystalline In_3Ni_2 sample, shown in Figure 2, cut along the (100) surface using a 50 micrometer thick tungsten wire saw. Boron carbide power in a glycerol suspension was used during this process to minimize the damage to the atomic surface. The surface was then polished with diamond pastes of decreasing grain size down to 0.25 micrometers. The surface was cleaned in UHV conditions by several repeated cycles of Ar ion sputtering for 30 minutes, with an average drain current of approximately 6 μA and subsequent annealing for between 1 and 3 hours, between 300°C and 560°C. An optical pyrometer was used to measure the

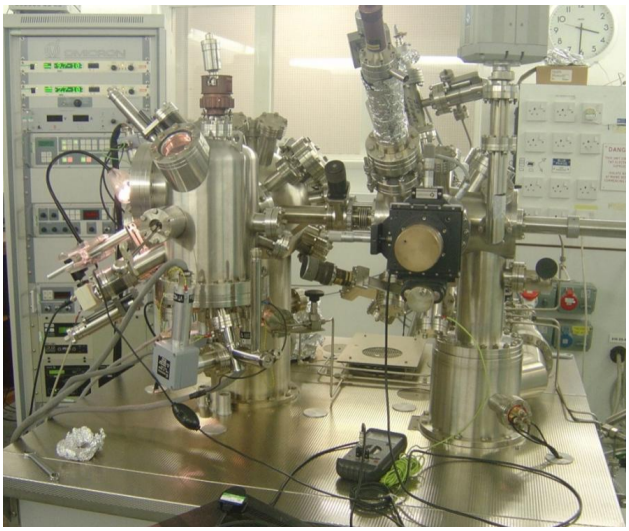

Figure 1: A UHV chamber.

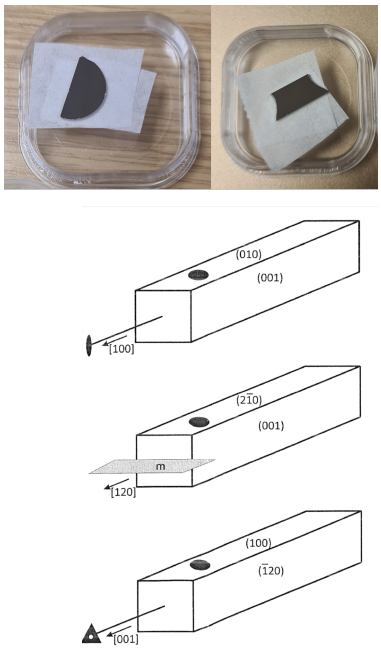

Figure 2: Images of the prepared sample of In_3Ni_2, and its surfaces.

temperature, however the emissivity for Ni-In was unknown so the emissivity of Ni-Cu was used instead[9]. This cycle was repeated until LEED patterns emerged. After preparation, by using XPS measurements, a lack of contamination on the atomic surface was affirmed.

The chamber used for preparation is directly connected to both STM and XPS chambers, so there was no change in surface conditions following the transfer of the sample to the STM chamber for measurements. LEED measurements were taken within the preparation chamber.

2.2 Scanning Tunneling Microscopy

Scanning tunneling microscopy is a method of imaging atomic surfaces using an atomically sharp metal tip brought approximately 0.5-1 nm away from a conducting surface. There is a voltage bias applied to the surface which allows electrons to tunnel through the vacuum barrier. The tunneling current is measured by the tip moving across the surface, and is proportional to the local density of state at the Fermi level. Information from the tunneling current is what is used to construct STM images, which then can be analysed to determine the structure of the surface atomic layer, which is useful to determine a number of factors such as planar termination or dimensions[11]. The STM images analysed for this report were taken at room temperature using an Omicron Variable Temperature STM in constant current mode ensuring consistent distance between the tip and the surface, and a bias voltage of 0.14-1.7 V was used. A diagram of an STM setup is shown in Figure 3.

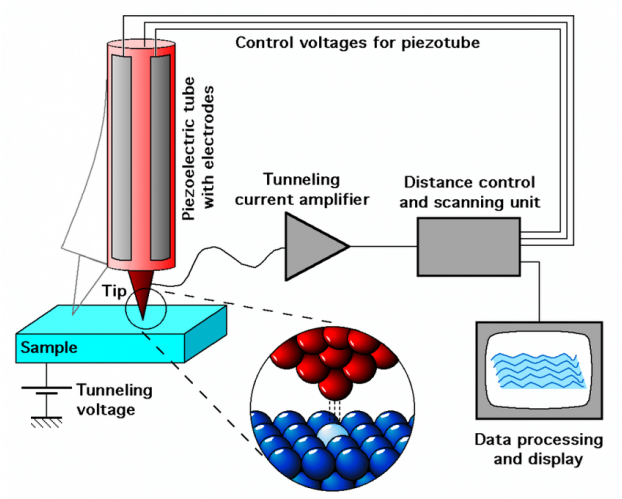

Figure 3: Diagram of the STM process, displaying the sharpness of the conducting tip, and the circuit used to control the tunneling current.

2.3 Low Energy Electron Diffraction

Low energy electron diffraction (LEED) is a technique which is used in surface science to analyse the crystal structure of the surface of a sample. As shown in Figure 4, low energy electrons are fired from an electron gun at the surface of a sample. The diffracted electrons are observed on a fluorescent screen at high voltage as spots of light known as a LEED pattern, which correspond to the surface's two dimensional reciprocal lattice[10]. The electron energies used are around 50 eV. At this energy, electrons are surface sensitive with minimal inelastic mean free path. This allows for high interaction with specifically the surface elements of the compound, which is necessary for imaging. Before accurate LEED patterns can be produced they must be calibrated with LEED patterns from known elements. The LEED patterns observed in this project were first calibrated with the Ag(100) surface.

2.4 X-ray Photoelectron Spectroscopy

X-ray photoelectron spectroscopy (XPS) is used to determine the chemical composition of an atomic surface. The basis of the technique is the photoelectric effect, wherein core-level electrons within an atom are ejected when an incoming x-ray exceeds their binding energy. By analysing the kinetic energy of the ejected electrons, binding energy can be calculated using the equation:

$$\text{BE} = h\nu \text{ - KE - } \phi$$

Where $h\nu$ is the energy of the incident x-ray photon, and ϕ is the work function of the spectrometer. As each element has a unique binding energy, elements present within a compound can be 'fingerprinted' and identified using this technique. XPS is only possible in UHV conditions, as otherwise there is a possibility of inelastic scattering of the photoelectrons[12]. An example of an

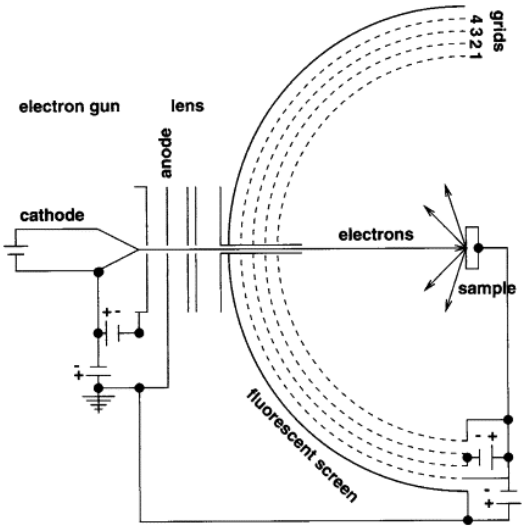

Figure 4: Diagram of the LEED process, displaying low energy electrons being emitted from an electron gun into the prepared sample.

XPS setup is shown in Figure 5. The XPS data used in this report was collected at the Institut Jean Lamour, France, using a nonmonochromatic Al K_α source. The oxidation process was carried out in UHV conditions by introducing 99.999% pure oxygen gas through a leak valve, and partial pressure was maintained at approximately 9.75 x 10^{-7} Torr. 99.99% pure molecular hydrogen was dosed on the prepared surface at room temperature.

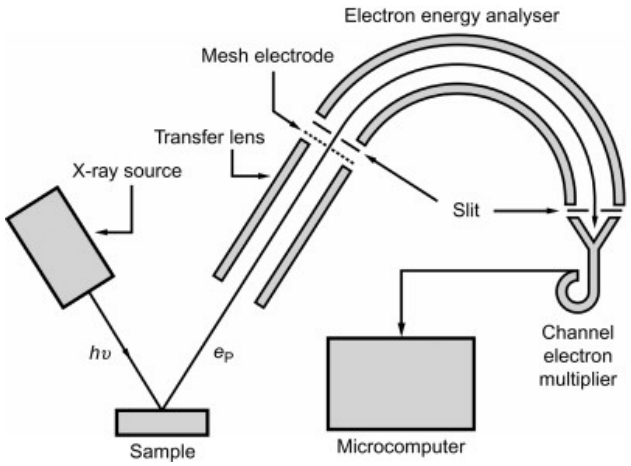

Figure 5: Diagram of the XPS process, displaying electrons reflecting off the prepared sample into an electron energy analyser to determine energy loss.

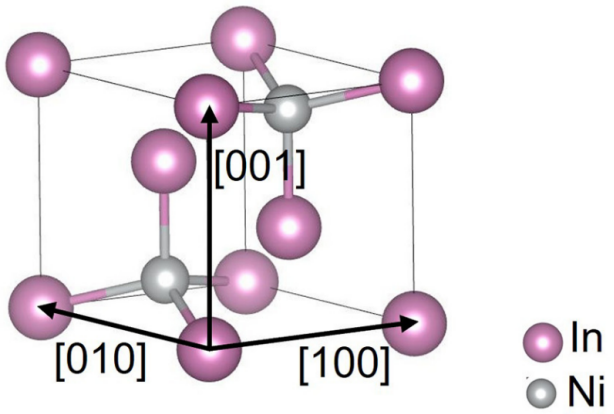

Figure 6: The unit cell of In_3Ni_2 [17].

2.5 Computational Details

A number of different programs were used in order to analyse the data required for this project. To determine the unit cell structure and dimensions from existing data, VESTA[13] was used. To analyse the STM data, WSxM[14] was used as it allows for the analysis of the height difference of inter-planar spacing, which allows for understanding of the 'step height' between the observed planes. Finally, CasaXPS[15] was used for analysis of the XPS data, which indicated peak position core levels and allowed for accurate chemical composition determination.

3 Results and Discussion

3.1 Crystal Structure

Shown in Figure 6 is the crystal structure of In_3Ni_2, the intermetallic compound. It has lattice parameters $a = b = 4.39$Å, $c = 5.30$Å and $\gamma = 90°$[16]. Each Ni atom is isolated by four In atoms. Figure 7 displays the side view of In_3Ni_2's (100) surface, with four atomic planes within a unit cell. The distance between each plane is equal, representing a third of the height of the unit cell. As each plane has equal distance, it is not possible to determine the termination plane using STM step height analysis, as it is not possible to differentiate between the content of atomic surfaces.

3.2 Surface Atomic Structure

3.2.1 STM - Step Height Analysis

By annealing the atomic surface from 420°C to 560° for an hour, a step-terrace morphology emerges that can be analysed using STM, as seen in Figure 8. For the data used in this report, the surface was annealed for longer to allow for larger terraces to emerge. The height of each step can be determined by using height distribution histograms and line scan graph analysis. Figure 9 displays an example of a height distribution histogram, where the distance between each peak represents a

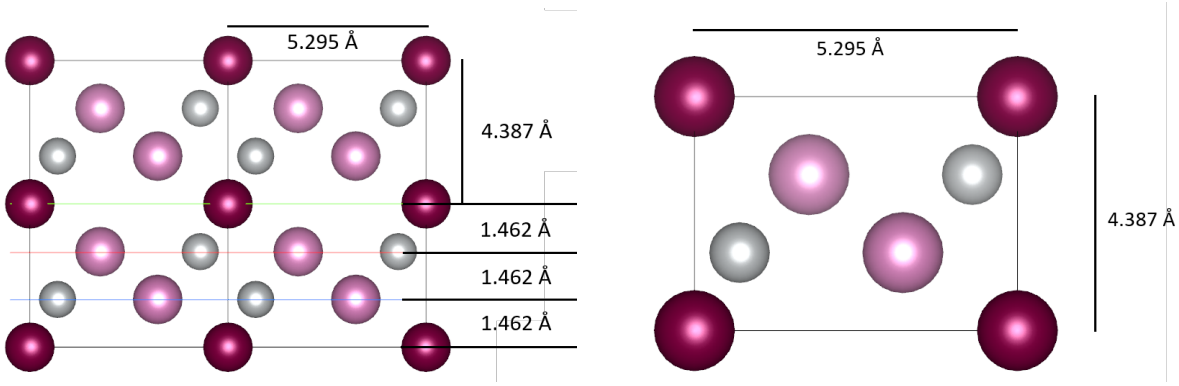

Figure 7: The side and top view of the (100) surface of the unit cell, with dimensions of the unit cell labeled, in addition to the planar spacing.

'step height', or distance between terraces. This process was repeated for thirteen images, wherein an average of the step height was measured.

Through this method, the values gathered for the different step heights were collected and compared to the previously discovered values. After measurement, eleven of the thirteen sets of measurements were found to be consistent with expected values. The most common step height was consistent with 4.44 Å, which represents the full unit cell height, which itself corresponds to separation of pure In planes. Step heights consistent with 2.96 Å were also found, which represent $\frac{2}{3}$ of the unit cell, however these were less frequent. Two results were not found to be consistent with expected values, however this is as a result of the low resolution of the images.

As observed in Figure 7, there is equal distance between each atomic plane of In_3Ni_2. Since the measured step heights could represent any combination of starting and termination planes, it is therefore not possible to categorically determine whether the atomic surface of In_3Ni_2 is a mixed Ni and In plane or a pure In plane through STM step height analysis alone. However, it is most likely from this data that the plane of termination is the pure In plane.

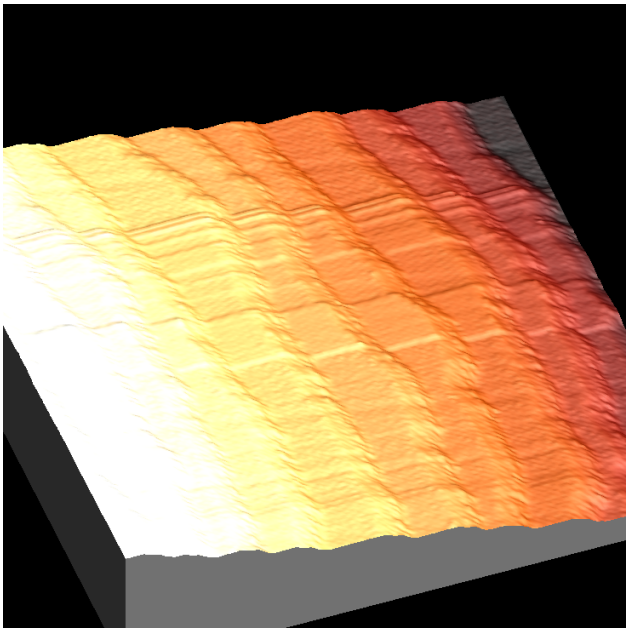

Figure 8: A 3D STM image of the (100) atomic surface of In_3Ni_2 displaying the different 'steps' produced by annealing at high temperatures.

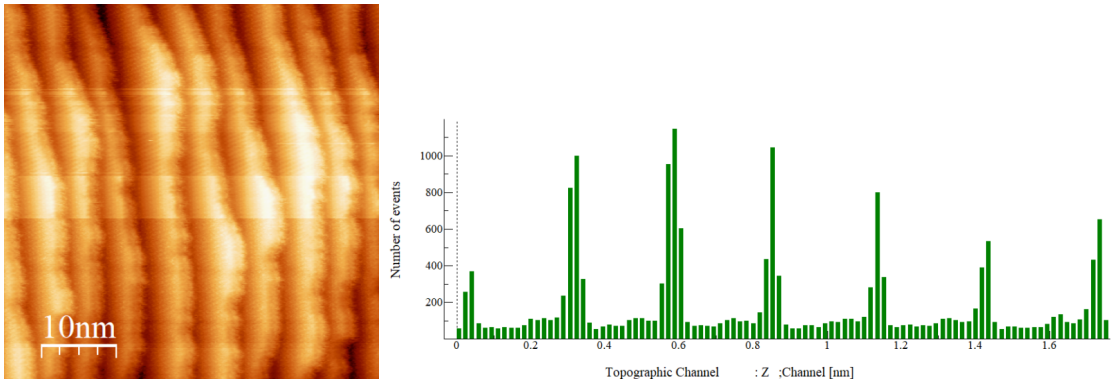

Figure 9: An example of a 2D STM image of In_3Ni_2 and a histogram, displaying the height distribution of a section of the image. The distance between each peak represents the distance between each observed terrace.

3.2.2 STM - Atomic Spacing Analysis

It is also possible to observe and calculate values for the atomic spacing of the (100) surface of In_3Ni_2 using STM imagery, in addition to directly measuring distance between atoms. This is possible by using either self-correlation or using a Fast Fourier Transform filter. As shown in Figure 10, high resolution images of the atomic surface can be taken, and while atomic resolution is somewhat observable in the raw image it is difficult to obtain accurate values through these alone. By applying self-correlation or a Fast Fourier Transform filter, the images can become similar to the image shown in Figure 11. Within this image, eat "dot" represents an atom, and therefore the distance between each can be measured to determine the atomic spacing.

By taking a line scan measurement of 10 different unit cells both horizontally and vertically, an average length for each unit cell measurement can be found. Unfortunately, some of the images analysed were of too low a resolution to reliably determine measurements for the unit cell lengths in the horizontal direction. Furthermore, there was a "shift" observed in the measurements caused by the scanning nature of the image photographing. This causes the atoms to appear at an angle, meaning that the unit cell lengths were distorted and not representative of the true values. By using trigonometry and finding the angle between the shift and the "true" vertical and horizontal, corrected values for the unit cell lengths can be determined. The average values attained after correction were found as 4.40 ± 0.1 Å and 5.29 ± 0.1 Å. Both of these values are consistent with the separation of In atom in the In plane. These lattice parameters are consistent with the dimensions between In atoms from the top view of the (100) surface of In_3Ni_2 as seen in Figure 7.

These high resolution images and step-height distributions suggest that surface termination occurs with the pure Indium plane. This can be understood because In has lower surface free energy than Ni. The surface free energy of the close-packed surface of body-centered tetragonal In is 0.488 J/m^2, while that of the close-packed surface of face-centered cubic Ni is 2.011 J/m^2[18]. This suggests that the plane being observed and analysed is a pure In plane, as if the mixed In and Ni plane were being observed, the distance between atoms would be smaller. In the compound, the distance between neighbouring In atoms in the topmost layer is 4.387 Å. However, the distance between In atoms in the topmost layer and Ni atoms in the layer beaneath is 2.673 Å, indicating that there is a high likelihood that the In atoms are bonded with Ni. The potential Ni-In bonding is likely the reason behind the stability of the atomic surface, as has been observed in other binary intermetallics such as Zn-Pd[19] and the (001) surface of In_3Ni_2[17].

3.2.3 LEED

A number of LEED patterns were photographed after the atomic surface was annealed and sputtered at a range of temperatures, increasing incrementally from 300°C to 560°C, in an energy range of 10-100 eV. The images were captured with a digital charge-coupled camera and a data acquisition system controlled by a computer.

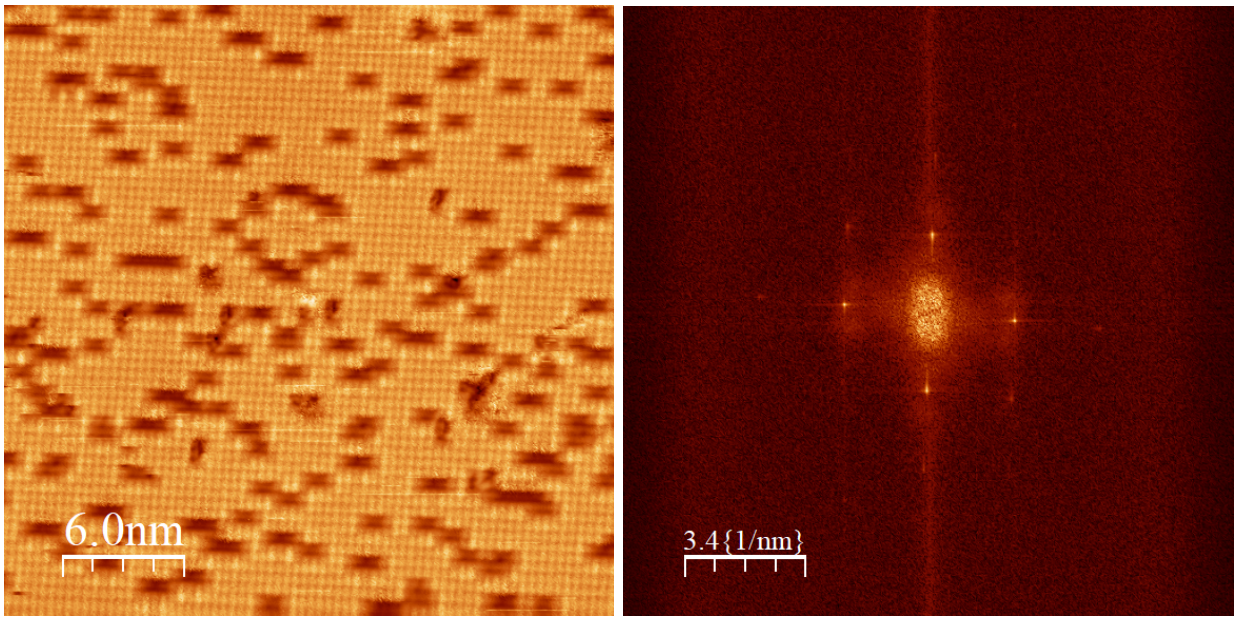

Figure 10: An example of an unfiltered high-resolution image of the (100) atomic surface of In_3Ni_2, and the same image when processed through a Fast Fourier Transform filter.

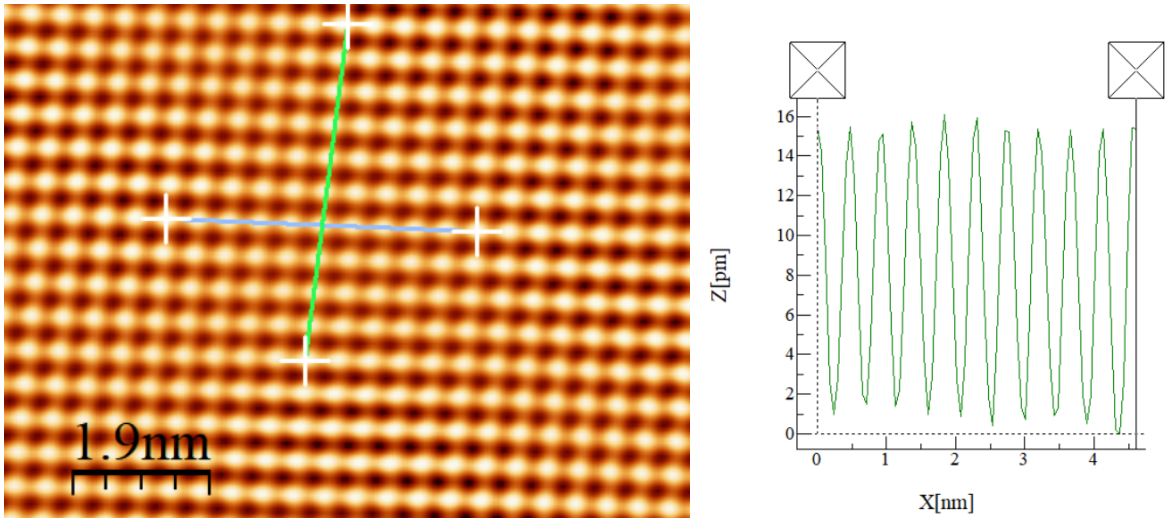

Figure 11: A high-resolution image of the (100) atomic surface of In_3Ni_2, with measuring lines spread across 10 unit cells vertically and horizontally, and an example of what a graph produced by this measurement looks like.

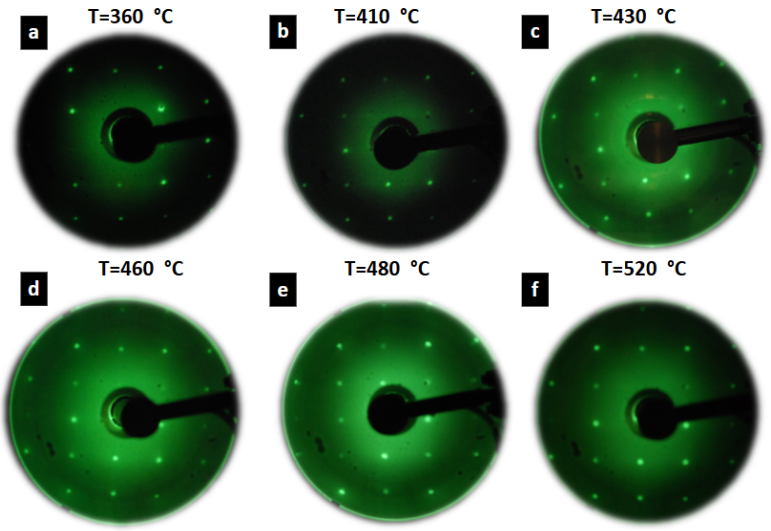

Figure 12: LEED patterns of In_3Ni_2 observed at a range of different temperatures.

No LEED pattern emerged within the temperature range of 300-360°C, as the temperature is not sufficient to produce perfect surface ordering. After 360°C, the surface began to exhibit a (1 x 1) LEED pattern with a rectangle-shaped structure. This is consistent with the other measurements taken with STM atomic resolution analysis as well as known measurements of the unit cell dimensions and angles.

Figure 12 displays the observed LEED patterns at a variety of temperatures. The pattern is most clearly observed at temperatures between 430-480°C, indicating that this is the ideal temperature for surface ordering. The observed shape and pattern is consistent with expected values and understanding of the lattice parameters. Additionally, Figure 13 displays observed LEED patterns at a range of beam energies between 20-100 eV. The observed pattern becomes more defined the greater the energy of the beam, though there are diminishing returns following approximately 60 eV. The shape and pattern produced through this method is also consistent with expectations and known values.

3.3 Surface Chemical Composition

3.3.1 XPS

To determine the chemical composition of the (100) surface of In_3Ni_2, XPS was used. An example of a spectra is shown in Figure 14. Integrating the measured intensity of the the In $3d_{5/2}$ and Ni $2p_{3/2}$ peaks within the XPS spectra at a range of angles between 0-70° allows for determination of the atomic composition observed. The measurements were taken after the atomic surface was annealed and sputtered at 560°C. By analysing this data, it can provide an indication of which ele-

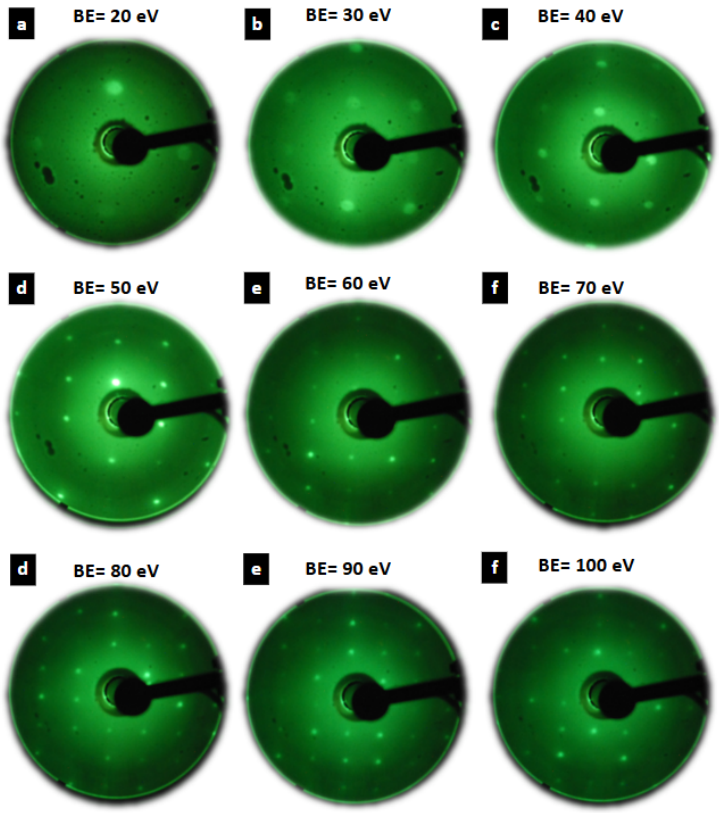

Figure 13: LEED patterns of In_3Ni_2 observed at a range of different beam energies.

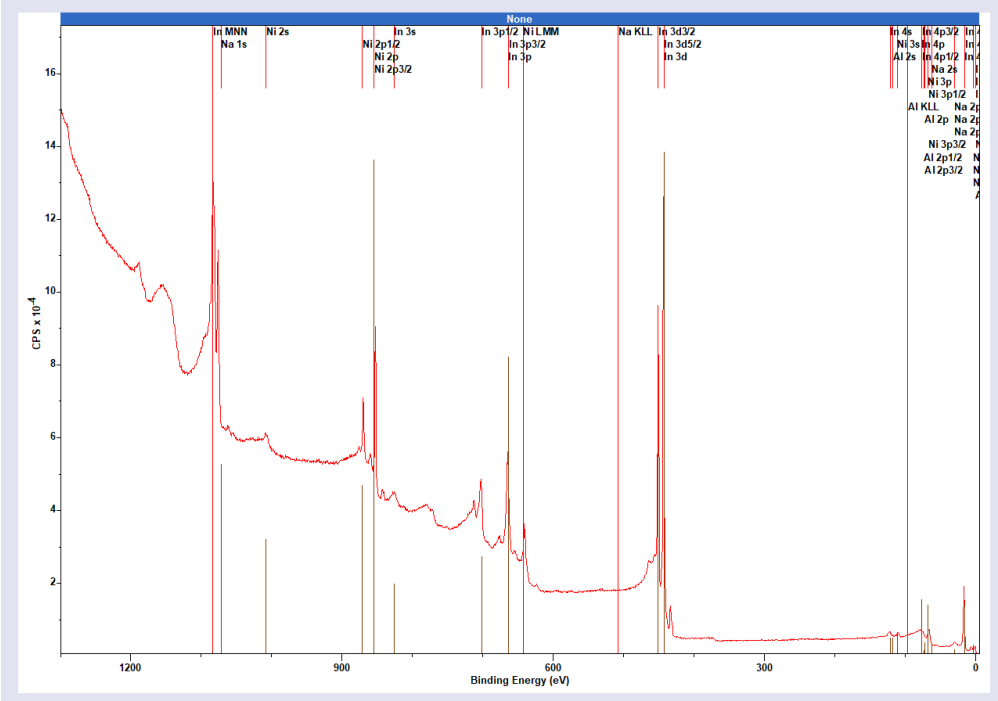

Figure 14: The XPS spectra for In_3Ni_2 at 0°. By measuring the area beneath the relevant peaks, atomic composition of the surface layers can be deduced.

ment preferentially segregates to the surface and thus gives a clearer indication of which materials are more present in the upper layers of the compound. Shallow angles, such as around 15°, do not penetrate far into the substance (around 1-2 nm) and therefore indicate which elements are present nearer the surface. Steeper angles up to 90° collect electrons from deeper within the compound. Distinguishing between the two and observing trends is vital to understand if the sputter-anneal process reveals one type of atom preferentially to the other.

Figure 15 represents the findings of this data. The dotted blue and red lines indicate the bulk composition of Ni and In respectively. The measured atomic compositions display that the proportion of Ni present at the surface is significantly higher than in the bulk. This is optimistic, as it indicates that the (100) surface of In_3Ni_2 contains a higher proportion of Ni, which is the more catalytically active element.

4 Summary

I investigated the atomic structure and chemical composition of the (100) surface of the intermetallic compound In_3Ni_2, using scanning tunneling microscopy (STM), low-energy electron diffraction (LEED), and x-ray photoelectron spectroscopy (XPS). The LEED patterns observed displayed a surface symmetry of (1 x 1), which was reinforced by high-resolution imaging of the atomic surface through STM images following transformation using self-correlation or a Fast Fourier Transform

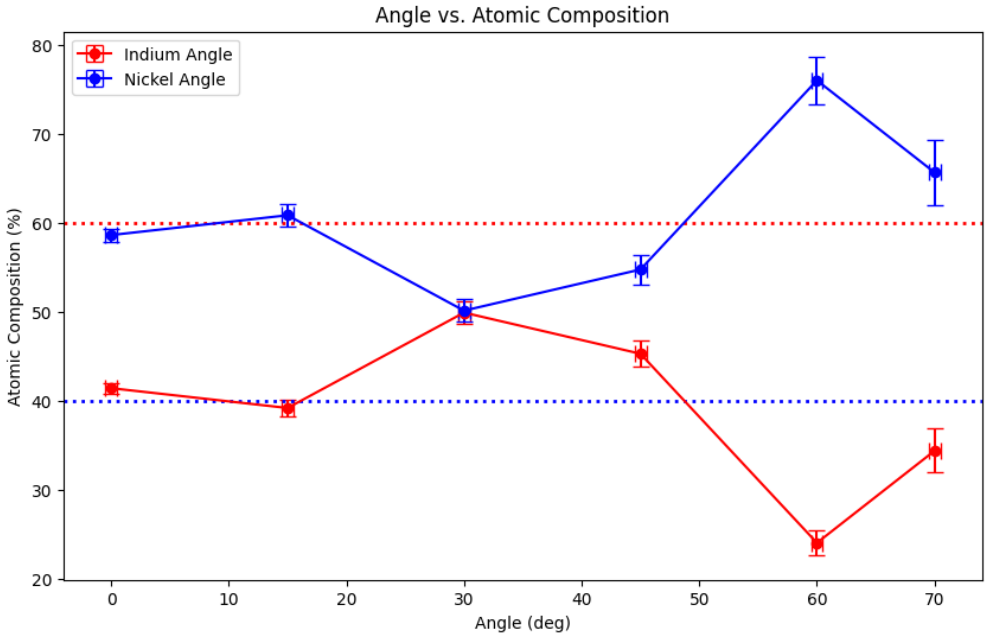

Figure 15: The chemical composition of the (100) surface of In_3Ni_2 at a variety of measured angles. The atomic composition was measured using the integrated intensity of the In $3d_{5/2}$ and Ni $2p_{3/2}$ peaks observed in the x-ray photoelectron spectroscopy spectra. The bulk composition of In is represented by the red dotted line, and the composition of Ni is represented by the blue dotted line.

filter. Analysing the planar distances of the step-terrace morphology produced by annealing the atomic surface at high temperatures indicated it is most likely that the termination surface is the pure In plane. This is as a result of the most common step height being a full unit cell length, indicating termination between stable planes. Furthermore, atomic resolution analysis of the atomic surface revealed spacing consistent with the atomic spacing between In atoms, further indicating the termination plane is pure In. XPS analysis of angle dependency suggested that the (100) surface of In_3Ni_2 has a notably higher proportion of Ni than the bulk composition after annealing at 560°C, indicating that it has promising potential as a catalyst due to the high composition of the more catalytically active element.

4.1 Future Work

In this project I attempted to determine the termination In_3Ni_2 using STM, but results could not be entirely verified as a result of the uniform planar distances. In future, low-energy ion scattering could be used to provide a clearer picture of the chemical composition of the very surface layer, indicating whether it is composed of pure In or mixed Ni and In.

5 Bibliography

1. M. Armbrüster, R. Schlögl, and Y. Grin. Intermetallic compounds in heterogeneous catalysis—a quickly developing field. Sci. Technol. Adv. Mater. **15**, 034803 (2014). https://doi.org/10.1088/1468-6996/15/3/034803

2. M. Armbrüster, M. Behrens, K. Föttinger, M. Friedrich, E. Gaudry, S. K. Matam, and H. R. Sharma. The Intermetallic Compound ZnPd and Its Role in Methanol Steam Reforming. Catal. Rev. **55**, 289 (2013). https://doi.org/10.1080/01614940.2013.796192

3. M. Armbrüster, K. Kovnir, M. Behrens, D. Teschner, Y. Grin, and R. Schlögl. Pd-Ga Intermetallic Compounds as Highly Selective Semihydrogenation Catalysts J. Am. Chem. Soc. **132**, 14745 (2010) https://doi.org/10.1143/JPSJ.80.064801

4. Z. Hou, M. Hua, Y. Liu, J. Deng, X. Zhou, Y. Feng, Y. Li, and H. Dai, Exploring Intermetallic Compounds: Properties and Applications in Catalysis, Catalysts **14**, 538 (2024). https://doi.org/10.3390/catal14080538

5. W. Liu, L. Li, S. Lin, Y. Luo, Z. Bao, Y. Mao, K. Li, D. Wu, and H. Peng. Confined Ni-In intermetallic alloy nanocatalyst with excellent coking resistance for methane dry reforming. J. Energy Chem. **65**, 34 (2022). https://doi.org/10.1016/j.jechem.2021.05.017

6. C. Li, Y. Chen, S. Zhang, S. Xu, J. Zhou, F. Wang, M. Wei, D. G. Evans, and X. Duan. Ni–In Intermetallic Nanocrystals as Efficient Catalysts toward Unsaturated Aldehydes Hydrogenation. Chem. Mater. **25**, 3888 (2013). https://doi.org/10.1021/cm4021832

7. J. P. Hobson, Methods of Producing Ultrahigh Vacuums and Measuring Ultralow Pressures, pp. 187–215 (Oxford University Press, Oxford, **1967**). https://doi.org/10.1007/978-1-4615-7969-4_5

8. J. F. O'Hanlon, A User's Guide to Vacuum Technology, 3rd ed., pp 379-402 (Wiley-Interscience, New York, **2003**). https://doi.org/10.1002/0471467162

9. https://ennologic.com/wp-content/uploads/2018/07/Ultimate-Emissivity-Table.pdf

10. M. A. Van Hove, W. H. Weinberg, and C.-M. Chan, Low-Energy Electron Diffraction: Experiment, Theory and Surface Structure Determination (Springer-Verlag, Berlin, 1986). https://doi.org/10.1007/978-3-642-82721-1

11. G. Binnig and H. Rohrer, Scanning tunneling microscopy—from birth to adolescence, Rev. Mod. Phys. **59**, 615 (1987). https://doi.org/10.1103/RevModPhys.59.615

12. N. Gopala Krishna and J. Philip, Review on surface-characterization applications of X-ray photoelectron spectroscopy (XPS): Recent developments and challenges, Appl. Surf. Sci. Adv. **12**, 100332 (2022). https://doi.org/10.1016/j.apsadv.2022.100332

13. K. Momma and F. Izumi, VESTA3 for three-dimensional visualization of crystal, volumetric and morphology data, J. Appl. Crystallogr. **44**, 1272–1276 (2011). https://doi.org/10.1107/S0021889811038970

14. I. Horcas, R. Fernández, J.M. Gómez-Rodríguez, J. Colchero, J. Gómez-Herrero, and A.M. Baró, WSXM: A software for scanning probe microscopy and a tool for nanotechnology, Rev. Sci. Instrum. **78**, 013705 (2007). https://doi.org/10.1063/1.2432410

15. N. Fairley, V. Fernandez, M. Richard-Plouet, C. Guillot-Deudon, J. Walton, E. Smith, D. Flahaut, M. Greiner, M. Biesinger, S. Tougaard, D. Morgan, and J. Baltrusaitis, Systematic and collaborative approach to problem solving using X-ray photoelectron spectroscopy, Appl. Surf. Sci. Adv. **5**, 100112 (2021). https://doi.org/10.1016/j.apsadv.2021.100112

16. https://next-gen.materialsproject.org/materials/mp-21385

17. A. Y. Alfahad, V. K. Singh, E. Gaudry, J. Ledieu, V. Fournée, P. Gille, A. M. Gardner, P. R. Chalker, R. McGrath, and H. R. Sharma, Atomic structure, chemical composition, and oxidation behavior of the (001) surface of In_3Ni_2 intermetallic catalyst, Phys. Rev. Mater. **9**, 035801 (2025). https://doi.org/10.1103/PhysRevMaterials.9.035801

18. L. Vitos, A.V. Ruban, H.L. Skriver, J. Kollár, The surface energy of metals in the embedded-atom method, Surf. Sci. 411, 186–202 (1998). https://doi.org/10.1016/S0039-6028(98)00363-X

19. M. Lowe, A. Al-Mahboob, D. Ivarsson, M. Armbrüster, J. Ardini, G. Held, F. Maccherozzi, A. Bayer, V. Fournée, J. Ledieu, J.T. Sadowski, R. McGrath, H.R. Sharma, Atomic structure

of different surface terminations of polycrystalline ZnPd, Phys. Rev. Mater. 8 (2024) 105801. https://doi.org/10.1103/PhysRevMaterials.8.105801

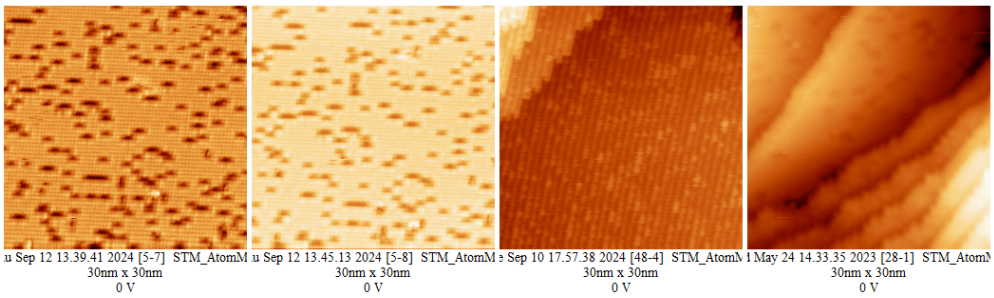

Figure 16: A number of STM images used during analysis.

6 Appendix

6.1 Project Proposal (submitted Week 2)

Tom Bonnar PHYS379 Project Outline
Intermetallic compounds have been found to possess optimistic properties in use as heterogeneous catalysis and coating, both of which can be attributed to surface phenomena. To ensure that these properties are most effectively utilised, it is vital to understand how they operate on an atomic scale by collecting and analysing data. My project will be to analyse the surface of the (100) Ni2In3 IMC and obtain necessary information to better understand its surface structure and chemical composition. I will use scanning tunnelling microscopy (STM), low-energy electron diffraction (LEED), and x-ray photoelectron spectroscopy (XPS) to characterise the surface atomic structure of the IMC.

6.2 Project Description

A number of techniques to investigate the atoms on the surface of an Indium-Nickel intermetallic compound were used. The goal was to find the type of atoms on the very surface layer. If Nickel, which is good for catalytic reactions, was found, it means that the compound has optimistic properties as a replacement for more expensive and less environmentally friendly metal catalysts currently being used. It was determined that Nickel was not present on the topmost layer, but is closely bonded to the surface atoms. This suggests that the compound being investigated has properties we were hoping to find during this investigation.

6.3 STM Images

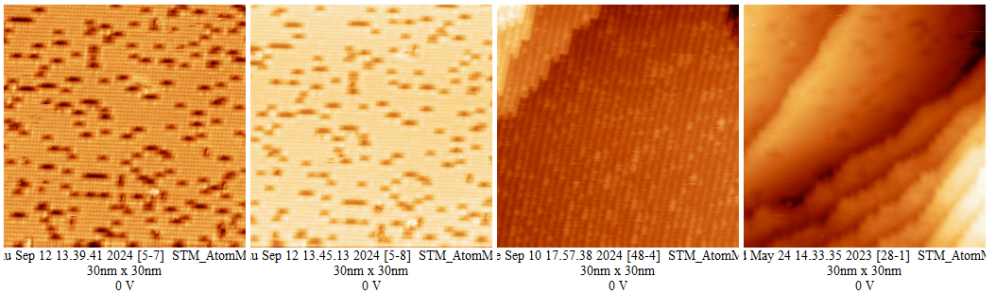

Figure 17: A number of STM images used during analysis.

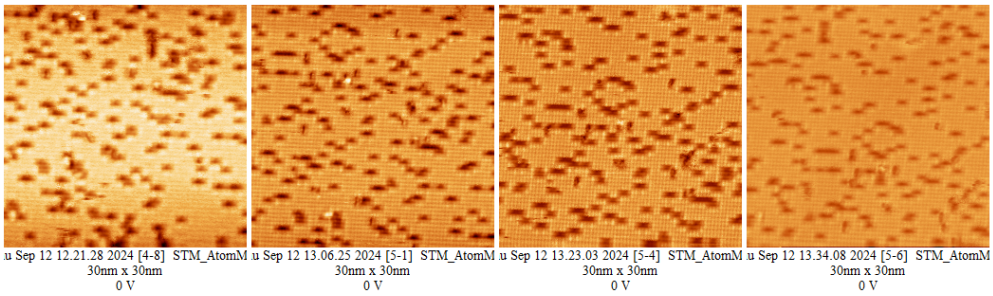

Figure 18: A number of STM images used during analysis.

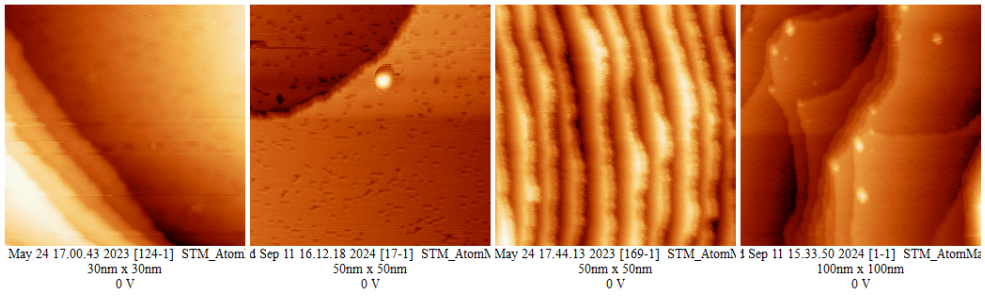

Figure 19: A number of STM images used during analysis.

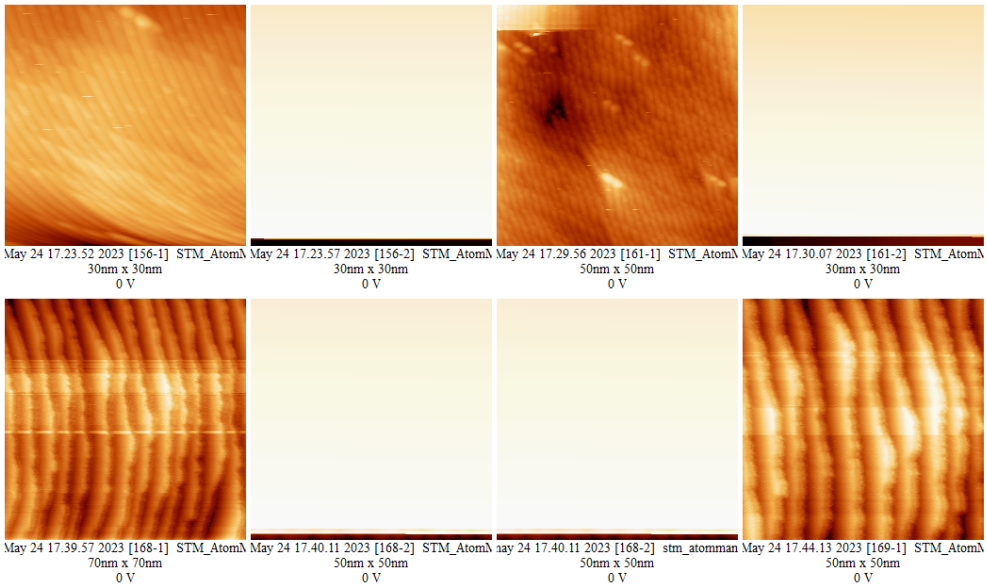

Figure 20: A number of STM images used during analysis.

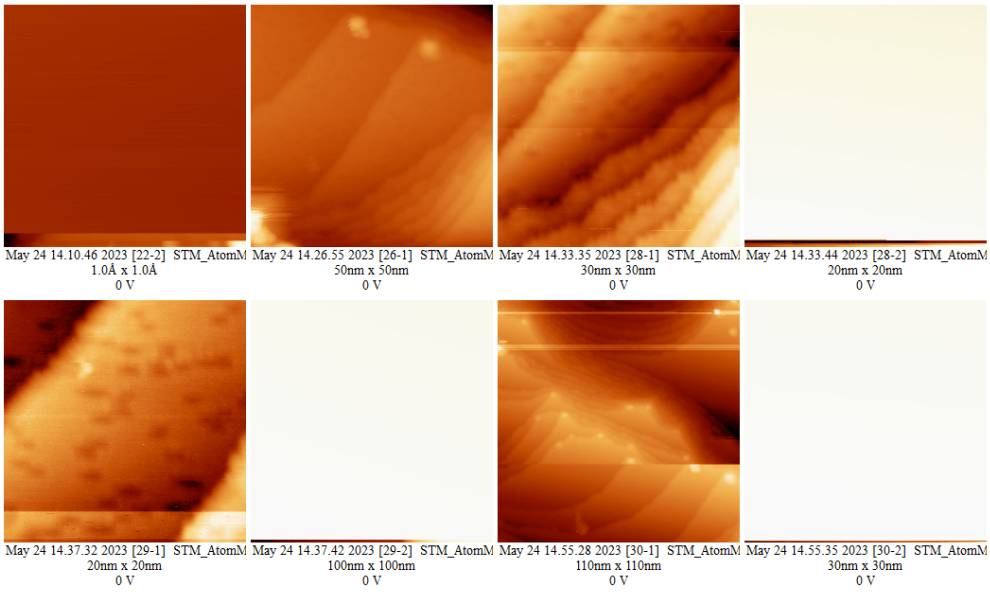

Figure 21: A number of STM images used during analysis.

6.4 Tables

vertical	5.29	5.3	5.04	4.7	4.63	4.61	4.61	4.58
horizontal	unable to resolve	unable to resolve	unable to resolve	4.27	4.19	4.22	4.24	4.15

Figure 22: Atomic spacing raw data.

Step Heigh	Image 1	Image 2	Image 3	Image 4	Image 5	Image 6	Image 7	Image 8	Image 9	Image 10	Image 11	Image 12	Image 13
1	0.236	0.234	0.411	0.4	0.389	0.405	0.299	0.219	0.379	0.207	0.34	0.371	0.416
2	0.229	0.231	0.415	0.398	0.376	0.42	0.283	0.228	0.385	0.223	0.334	0.385	0.373
3	0.224	0.235	0.415	0.382	0.373	0.407	0.275	0.216	0.382	0.236	0.337	0.395	0.39
4	0.238	0.225	0.411	0.374		0.387	0.278	0.228	0.388	0.231	0.331	0.382	0.37
5	0.239			0.376		0.415	0.283	0.222			0.323		
6				0.382		0.387	0.275	0.212			0.343		
7				0.376			0.278	0.219			0.334		
8							0.283	0.222					
9								0.225					
avg	0.2332	0.23125	0.413	0.384	0.379333	0.4035	0.28175	0.221222	0.3835	0.22425	0.334571	0.38325	0.38725
std	0.005776	0.003897	0.002	0.009914	0.006944	0.012672	0.007259	0.00505	0.003354	0.010986	0.00602	0.008555	0.018267
Corrected	0.269276	0.267024	0.476891	0.443405	0.438016	0.465922	0.325337	0.255445	0.442828	0.258942	0.38633	0.442539	0.447158

Figure 23: Step height analysis raw data.

Angle	Error	In 3d	Error	Ni 2p	Error
0	0.5	41.39	0.6	58.61	0.73
15	0.5	39.16	0.95	60.84	1.24
30	0.5	49.89	1.26	50.11	1.26
45	0.5	45.26	1.5	54.74	1.68
60	0.5	23.99	1.35	76.01	2.68
70	0.5	34.35	2.47	65.65	3.64

Figure 24: XPS analysis results table.